สำนักงานวิทยทรัพยากร
จุฬาลงกรณ์มหาวิทยาลัย

CHAPTER V
POLYLACTIDE/MAGNETIC MODIFIED MESOPOROUS CLAY NANOCOMPOSITES FOR FOOD PACKAGING

5.1 Abstract

Polylactide/Magnetic modified mesoporous clay nanocomposites were prepared via direct melt intercalation by twin screw extruder. Polycarprolactone was used as a compatibilizer to improve the dispersion of magnetic PCHs in PLA matrix. The PCHs were synthesized by the self-assembly of silica framework around surfactant templates intercalated within the galleries of Na-bentonite clay to obtain PCH which had the molar ratio of dodecylamine/TEOS was 20/200 before it was modified the surface by 20%wt ferric chloride hexahydrate. After obtaining the magnetic PCHs, these magnetic porous materials were utilized as the inorganic filler in PLA nanocomposites. Subsequently, they were fabricated to thin sheet by compression molding machine. The nanocomposites were characterized by using XRD, DSC and TG-DTA. The T_g and T_m of PLA/5% wt PCL were lower than neat PLA. The thermal properties of PLA/5%wt PCL/1-4%wt Magnetic PCH nanocomposites increased with content of magnetic PCH. The PLA nanocomposite showed lower the oxygen gas permeability rate than neat PLA and PLA/5% wt PCL, respectively due to gas barrier properties of the magnetic PCH providing tortuous path in the films owing to mesoporous materials.

keyword : porous clay heterostructures, polylactide, nanocomposites.

5.2 Introduction

Among the renewable source-based biodegradable plastics, polylactides or poly(lactic acid) (PLA) is one of the most promising materials since it is thermoplastic, biodegradable, biocompatible and has high-strength, high-modulus and good processability [1]. PLA is a linear aliphatic thermoplastic which can either be synthesized by condensation of lactic acid or ring opening polymerization of lactide which is produced by fermentation of dextrose which it self is gained from annually renewable resources like corn [2]. The growth of environmental concerns

over non-biodegradable petrochemical based plastic packaging materials has raised interest in the use of biodegradable alternatives originating from renewable sources [3-4].

Recently, there has been a growing interest in the development of polymer-clay nanocomposites. Nanocomposites constitute a new class of material that involves nano-scale dispersion in a matrix. Nanocomposites have at least one ultrafine phase dimension, typically in the range of 1–100 nm, and exhibit improved properties when compared to micro- and macro-composites. Strong interfacial interactions between the dispersed clay layers and the polymer matrix lead to enhanced mechanical, thermal and barrier properties of the virgin polymer [6]. The most commonly used clay to prepare nanocomposite is from the smectite group, such as montmorilonite (MMT). In this clay mineral the silicate layers are joined through relatively weak dipolar and Van der Waals forces and the cations Na^{+} and Ca^{2+} located in the interlayers. These cations can be replaced by organic cations such as alkylammonium ions through an ionexchange reaction to provide an organophilic silicate. Nanocomposite can be obtained by direct polymer melt intercalation, where polymer chains are spread into the space between the clay layers and this can be done by conventional polymer processing techniques such as extrusion [7].

Many research efforts focus on the polylactide-clay nanocomposites. The nanocomposites were prepared by master batch method using a twin-screw extruder with poly(ε-caprolactone) (PCL) as a compatibilizer. The presence of org-MMT leads to obvious pseudo-solid-like behaviors of nanocomposite melts. Therefore, the storage moduli, loss moduli, and dynamic viscosities of PLACNs show a monotonic increase with MMT content. Nonterminal behaviors exists in PLACNs nanocomposites. Besides the PLACNs melts show a greater shear thinning tendency than pure PLA melt because of the preferential orientation of the MMT layers. Therefore, PLACNs have higher moduli but better processibility compared with pure PLA [9].

Recently, Nanocomposite technology paves the way for packaging innovation in the flexible film industries, offering enhance properties such as greater barrier protection, increased shelf life and lighter-weight material. From this point of view, one of the goals of this work is to study the % wt magnetic PCHs in PLA

matrix, these as-synthesized mesoporous materials were blended with polylactide, and the properties concerning the capability of polylactide–magnetic PCHs nanocomposites in food packaging and magnetic sensor were investigated.

5.3 Experimental

Materials

Na-Bentonite (BTN), (Mac-Gel® GRADE SAC), was obtained from Thai Nippon Chemical Industry Co., Ltd. The cation exchange capacity (CEC) of BTN is 55 mmol/100g of clay.

Cetyltrimethylammonium [$C_{16}H_{33}N^{+}(CH_3)_3$] bromide (CTAB) was supplied by Fluka. Dodecylamine, $C_{12}H_{27}N$, (98% purified) was supplied by Aldrich. Tetraehtyl orthosilicate (TEOS), Ammonium hydroxide (NH_4OH) and Ferric chloride hexahydrate ($FeCl_3.6H_2O$) were purchased from Fluka. Methanol (CH_3OH) was supplied by Lab Scan and Hydrochoric acid (HCl) was supplied by Carlo Erba.

Polylactide 4042D (PLA) was supplied by NatureWorks Co., Ltd and Polycaprolactone was supplied by Aldrich.

Purification and pH Adjustment of Bentonite

Bentonite was pulverized and sieve through 325 mesh. Four 10-g of the passing part were purified by centrifugation and then washed with distilled water several time until pH value was near 7. After that, centrifugation was applied. Again, the same amount of distilled was added, and then the sample was adjusted to pH 9.0 by using dilute HCl and NaOH solutions. The samples were air-dried overnight and pulverized in a mortar.

Synthesis of Porous Clay Heterostructures (PCHs)

The bentonite was converted into a quaternary ammonium exchange form by ion exchange with cetyltrimethylammonium bromide and stirred at 50°C for 24 h. After the reaction time, the solid was filtered out, washed with a mixture of methanol and water and then air-dried. The obtained organoclay was stirred in dodecylamine for 30 min at 50°C following which TEOS was added and study the molar ratio of dodecylamine/TEOS for clay 1 g. The resulting suspension was stirred for further 4 h at room temperature. The solid was separated from solution by filtration and air-dried overnight at room temperature to form the as-synthesized PCH. The surfactant was removed from the as-synthesized PCH using

methanol/HCL solution. Typically, 1 g of the as-synthesized PCH material has been added to 45 mL of methanol and 5 mL of HCl and refluxed for 2 h. The solid was subsequently filtrated out mixture of methanol and water and air-dried at room temperature overnight. The PCH was obtained.

Preparation of Magnetic PCHs

Ferric chloride hexahydrate was used as iron sources which it was added in PCH at 0,5,10,15,20 wt%. Aqueous ammonia was used as the precipitator. Distilled water was used as the solvent. Before the reaction, N_2 gas was flown through the reaction medium. The reaction was operated in a closed system to provide a nonoxidation environment. NH_4OH was slowly injected into PCH which added ferric chloride hexahydrate under stirring 30 min. The dispersion was centrifuged at 3000 rpm for 20 min. After precipitation, the Fe_3O_4 particles in PCH were repeatedly washed and filtered before drying at room temperature in air atmosphere to form powders.

Preparation of Nanocomposites

1, 2, 3, 4 wt% Magnetic Clay, 5 wt% PCL and PLA were melt blended in a Model T-20 co-rotating twin-screw extruder (Collin) with L/D=30 and D=25 mm; the processing conditions were the following: temperature (°C): 80, 150, 155, 160, 165, and 160°C from hopper to die, respectively and the screw rotation was 50 rpm. Each composition was premixed in a tumble mixer before introducing into the twin-screw extruder to be well mixed and extruded through a single strand die, and solidified with cold water and pelletized. The obtained pellet was dried in oven.

Fabrication of Thin Sheet Nanocomposites

The nanocomposites films were prepared by compression molding machine. The nanocomposites pellets were dried in oven prior to compress. The compression molding was performed by using a Wabash V50H Press, at 180°C for 15 minutes and 10 tons compression force for 3 minutes before being cooled down to 50°C and thickness in the range of 0.1–0.25 mm.

Physical Measurements

X-ray diffraction patterns were measured on a Rigaku Model Dmax 2002 diffractometer with Ni-filtered Cu K_α radiation operated at 40 kV and 30 mA. The nanoconposite films were observed on the 2θ range of 2-20 degree with a scan speed of 5 degree/min and a scan step of 0.02 degree.

TG-DTA curves were collected on a Perkin-Elmer Pyris Diamond TG/DTA instrument. The sample was loaded on the platinum pan and heated from 30°C to 700°C at a heating rate of 10°C/min under N_2 flow.

DSC analysis were carried out using a Perkin-Elmer DSC 7 instrument. The sample was first heated from 30°C to 200°C and cooled down at a rate of 10°C/min under a N_2 atmosphere with a flow rate of 60 ml/min. The sample was then reheated to 200°C at the same rate.

Gas permeation experiments were investigated by Brugger Gas Permeability Tester. The sample films were cut into circular shape with 110 mm in diameter according to ASTM 1434-82. The thickness of the films was measured with the peacock digital thickness gauge model PDN 12N by reading ten points at random position over the entire test area and the results were averaged. The films were placed in a dessicator over NaCl and kept for not less than 3 days prior to test.

Scanning electron microscopy was performed on JSM 5800 LV Model. The specimens were coated with gold under vacuum to make them electrically conductive.

5.4 Results and Discussion

Porous clay heterostructure (PCHs) and Magnetic PCHs

PCH (D/T = 20/200) surface was modified by Fe ions (Fe^{2+} and Fe^{3+}), from the 20%wt ferric chloride hexahydrate for using as magnetic sensor. The results reveal that PCHs had surface areas of 609 m^2/g, average pore diameter of 5.35 nm, and pore volume of 0.82 cc/g, respectively while Magnetic PCHs had a result of 148 m^2/g, average pore diameter of 14.58 nm, and pore volume of 0.54 cc/g, respectively. The results of UV/vis absorbance spectra showed that the absorbance spectra of PCH, magnetic PCH (5–20%wt of Fe ion) and bentonite had the appearance of a broad band at 242 nm points to the charge transportation from O^{2-}, OH^-, or H_2O to the iron (Fe^{3+}) in the octahedral layer of the clay mineral. From SEM images and consistent EDX micrograph of Fe ion in PCH, the results showed that the incorporation of Fe ion in PCH is successful. Magnetic PCH exhibited a remarkably significant bacteriostatic effect against *Escherichia coli* and *Staphylococcus aureus*.

Thermal Properties of Nanocomposites

Melting temperatures of PLA and the nanocomposites are observed by DSC heating scan thermograms in Figure 5.1. The neat PLA showed a clear glass transition temperature(T_g) at 56.74°C and the melting temperature(T_m) of PLA was 149.00°C. The T_g and T_m of PLA/ 5%wt PCL which PCL acts as the compatibilizer and plasticizer decreased lower than neat PLA. After blending PLA with PCL as a compatibilizer, the T_g and T_m of PLA/ 5%wt PCL were lower than those of neat PLA. While the thermal properties of PLA/ 5%wt PCL /1–4%wt magnetic PCH nanocomposites increased as the higher content of added magnetic PCH. All results of thermal properties are listed in Table 5.1 and Figure 5.1–5.2.

Table 5.1 Thermal behavior of PLA and nanocomposites

Sample	T_g (°C)	T_m (°C)	T_d(°C)	Char residue at 600 °C
PLA	56.74	149.00	341.89	1.76
PLA/ 5%wt PCL	46.55	137.49	342.16	1.82
PLA/ 5%wt PCL/ 1%wt magnetic PCH	50.22	140.94	342.69	2.32
PLA/ 5%wt PCL/ 2%wt magnetic PCH	52.04	141.13	343.55	4.06
PLA/ 5%wt PCL/ 3%wt magnetic PCH	53.08	142.40	345.42	4.21
PLA/ 5%wt PCL/ 4%wt magnetic PCH	54.93	147.41	346.91	5.07

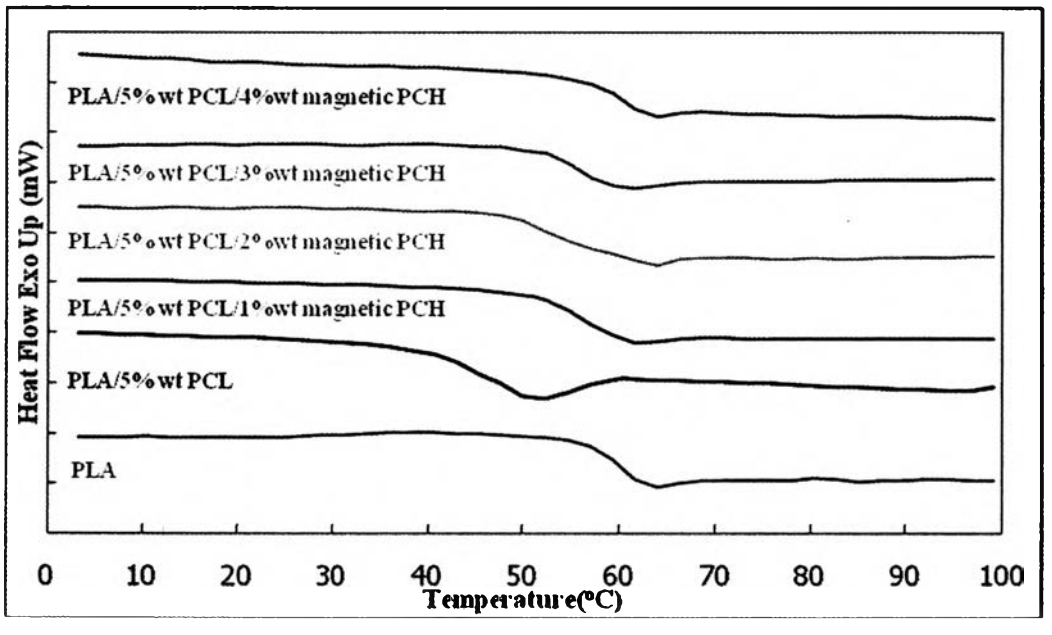

(a)

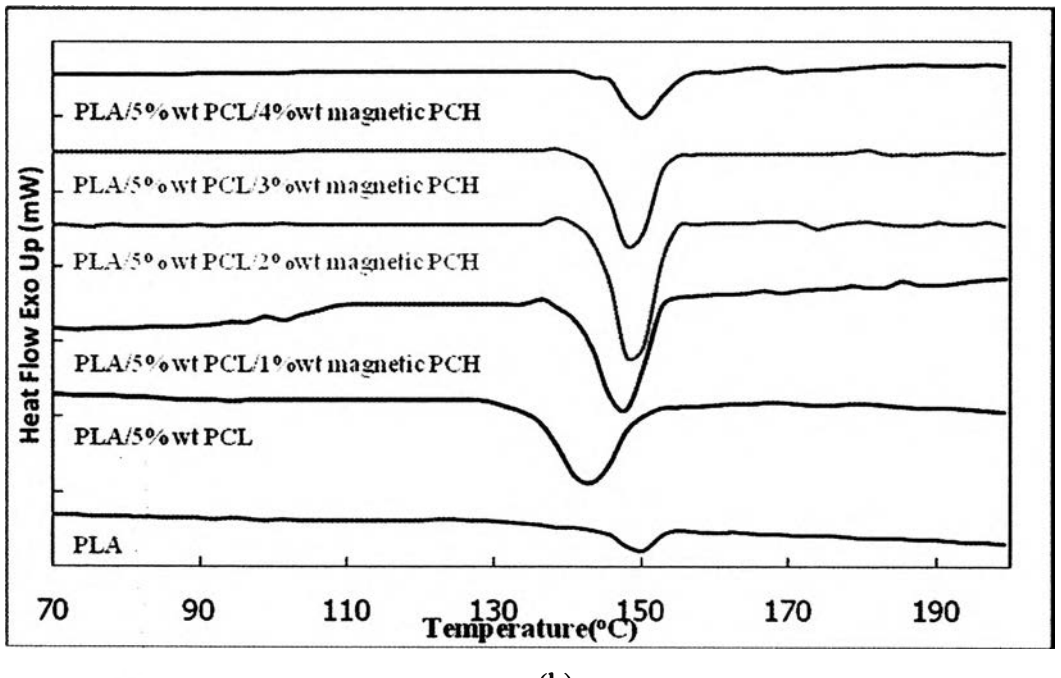

(b)

Figure 5.1 DSC heating scan thermograms of neat PLA, PLA/5%wt PCL and various magnetic PCH nanocomposites (a) Glass transition temperature and (b) Melting temperature.

TG-DTA curves of PLA and the nanocomposites are delineated in Figure 5.2. The thermal degradation of PLA and all nanocomposites occured in single stage, and it indicated that thermal stability of the nanocomposites were marginally increased when compared to that of neat PLA. Generally, the shift considerably towards higher temperature may be attributed to the formation of a high-performance carbonaceous-silicate char, builds up on the surface [16]. Despite all these, the results reveal that the addition of these porous materials just slightly improve the thermal stability of PLA which may be responsible for some destruction of clay layers on magnetic PCHs materials. So they could not dominate the thermal stability of PLA. However, the residue value of char were rather consistent with the amount of clay that had been added to the PLA.

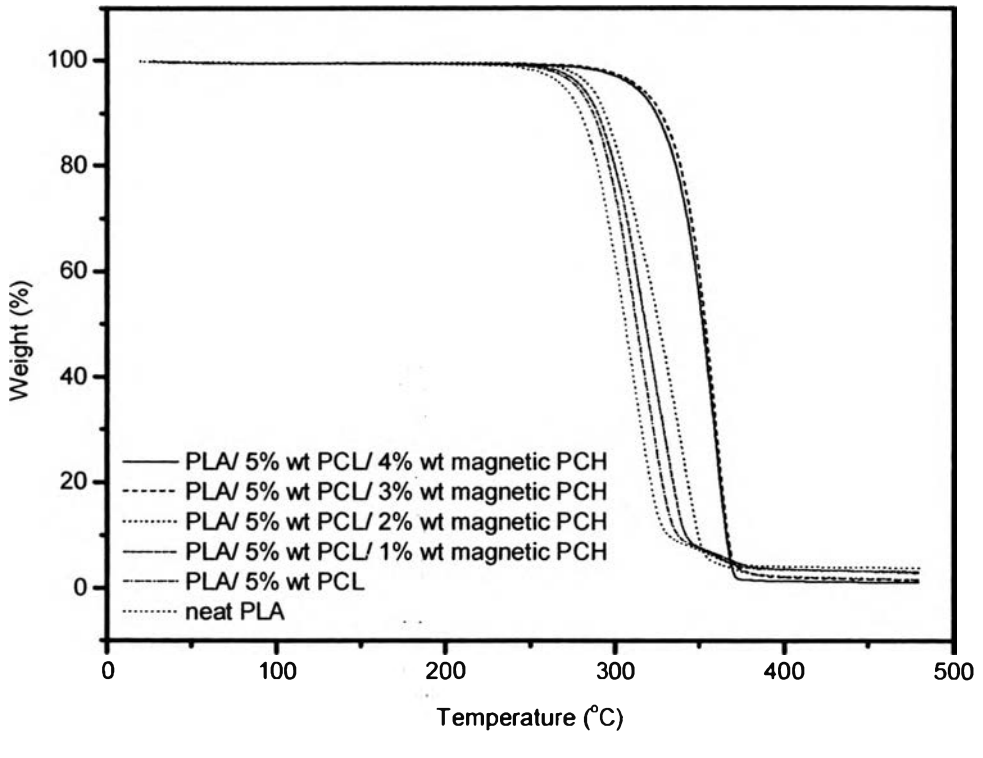

Figure 5.2 TG-DTA curves of neat PLA , PLA/5%wt PCL and various magnetic PCH nanocomposites.

Mechanical measurement of PLA nanocomposites

The mechanical properties of the PLA/ 5%wt PCL /1–4%wt magnetic PCH nanocomposites are shown in Table 5.2 and Figure 5.3 – 5.5. Tensile strength, young's modulus and % elongation at break decreased when the content of magnetic PCH increased. The aggregation of magnetic PCH affect to the mechanical properties of nanocomposites and the obstruction of magnetic PCH to the movement of PLA matrix was a reason in decline of mechanical properties with increasing magnetic PCH content which propably leads to lower polymeric chain mobility.

Table 5.2 Mechanical Properties of neat PLA and nanocomposites

Sample	Tensile Strength (MPa)	Elongation at Break (%)	Young's Modulus (MPa)
PLA	5.971 ± 0.2	6.475 ± 0.5	1431 ± 178
PLA/ 5%wt PCL	2.382 ± 0.1	5.908 ± 0.9	2106 ± 89
PLA/ 5%wt PCL/ 1%wt magnetic PCH	2.342 ± 0.2	5.826 ± 0.7	1981 ± 46
PLA/ 5%wt PCL/ 2%wt magnetic PCH	2.133 ± 0.2	5.697 ± 0.3	1940 ± 166
PLA/ 5%wt PCL/ 3%wt magnetic PCH	1.338 ± 0.2	3.541 ± 0.5	1744 ± 226
PLA/ 5%wt PCL/ 4%wt magnetic PCH	0.489 ± 0.4	2.662 ± 0.7	1721 ± 235

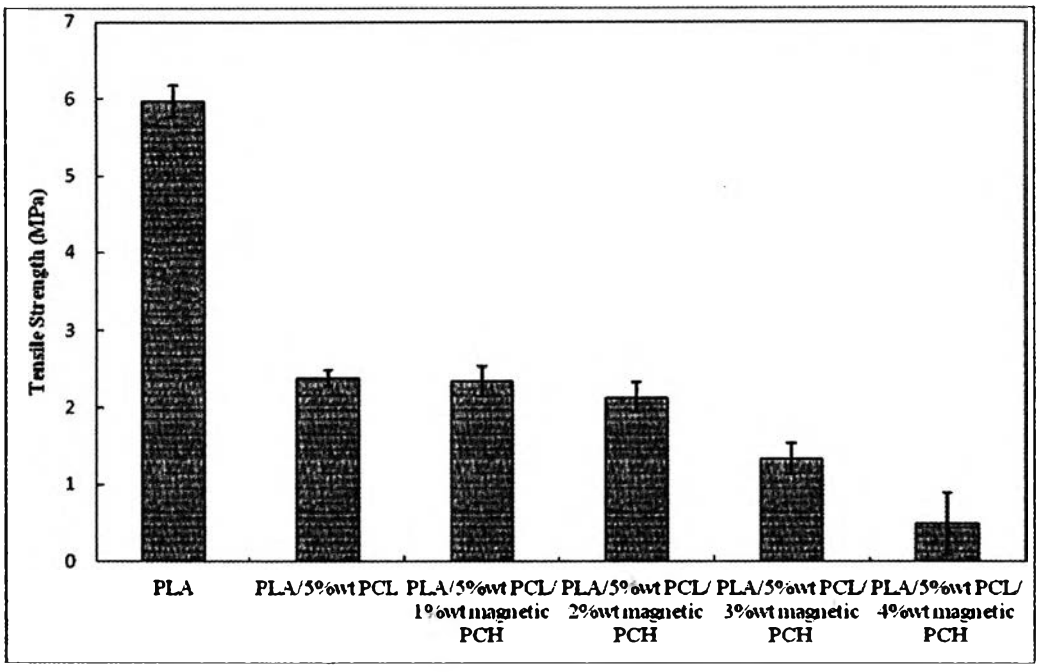

Figure 5.3 Tensile Strength of neat PLA, PLA/5%wt PCL and various magnetic PCH loading.

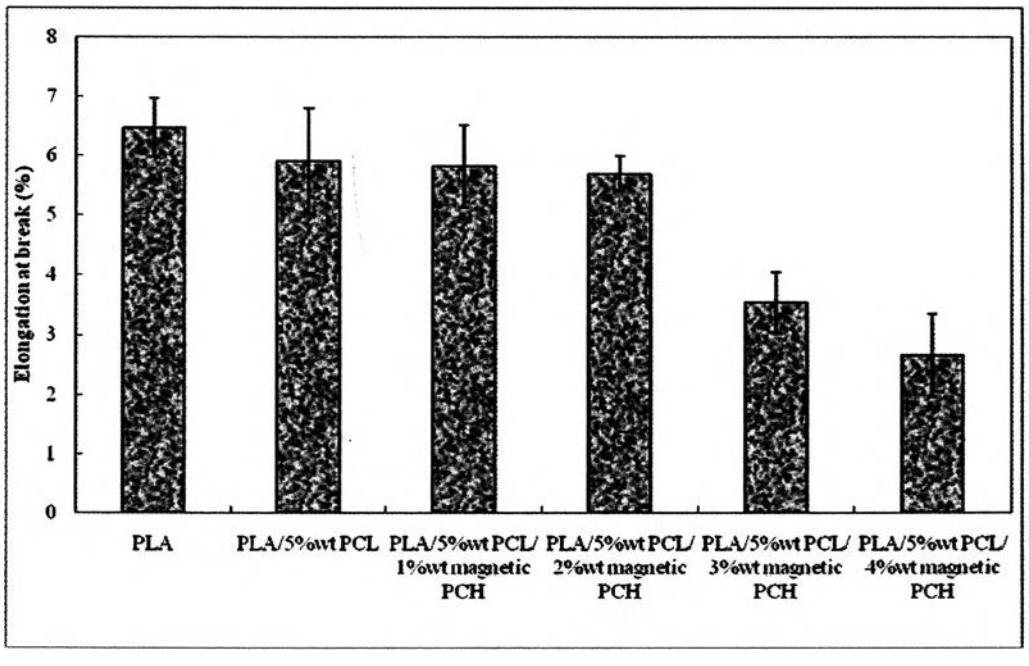

Figure 5.4 % Elongation at Break of neat PLA, PLA/5%wt PCL and various magnetic PCH loading.

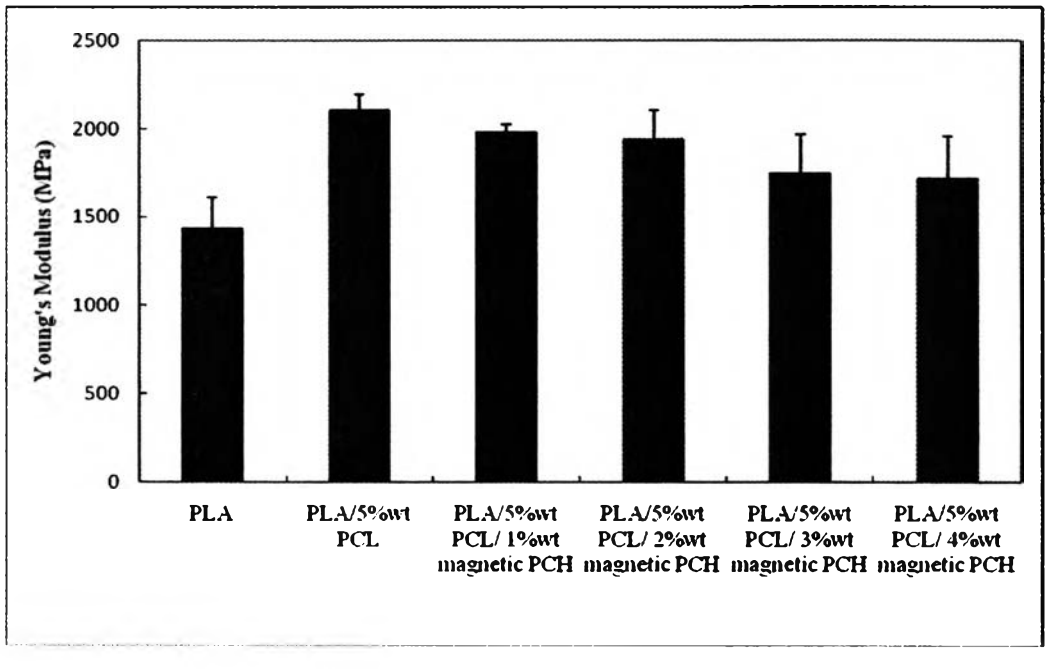

Figure 5.5 Young's Modulus of neat PLA, PLA/5%wt PCL and various magnetic PCH loading.

Elemental Composition of PLA Nanocomposite Films

EDX analysis indicates different chemical element composition of representative magnetic PCH nanocomposite films, which is presented in Table 5.3. The existence of much carbon is a normal attribute of PLA matrix. SEM images and consistent EDX micrographs of the representatives are demonstrated in Figure 5.6.. Bentonite was the host clay of magnetic PCH, was hydrated alumino silicates. It was comprised of a three layer structure with alumina sheets sandwiched between tetrahedral silica units. According to the EDX results, they reveal the distribution of C, Si, Al, O and Fe throughout the nanocomposite films, suggesting that the porous clays could be widely dispersed on PLA matrix, although their consistent SEM images exhibited clusters of the porous clays in some extent of the nanocomposites films.

Table 5.3 Element percentage of representative porous clay nanocomposite films

Sample	Selected Chemical Element (%Atomic)				
	C	Si	Al	O	Fe
PLA/5% wt PCL/1% wt magnetic PCH	57.51	2.72	0.04	38.7	1.03

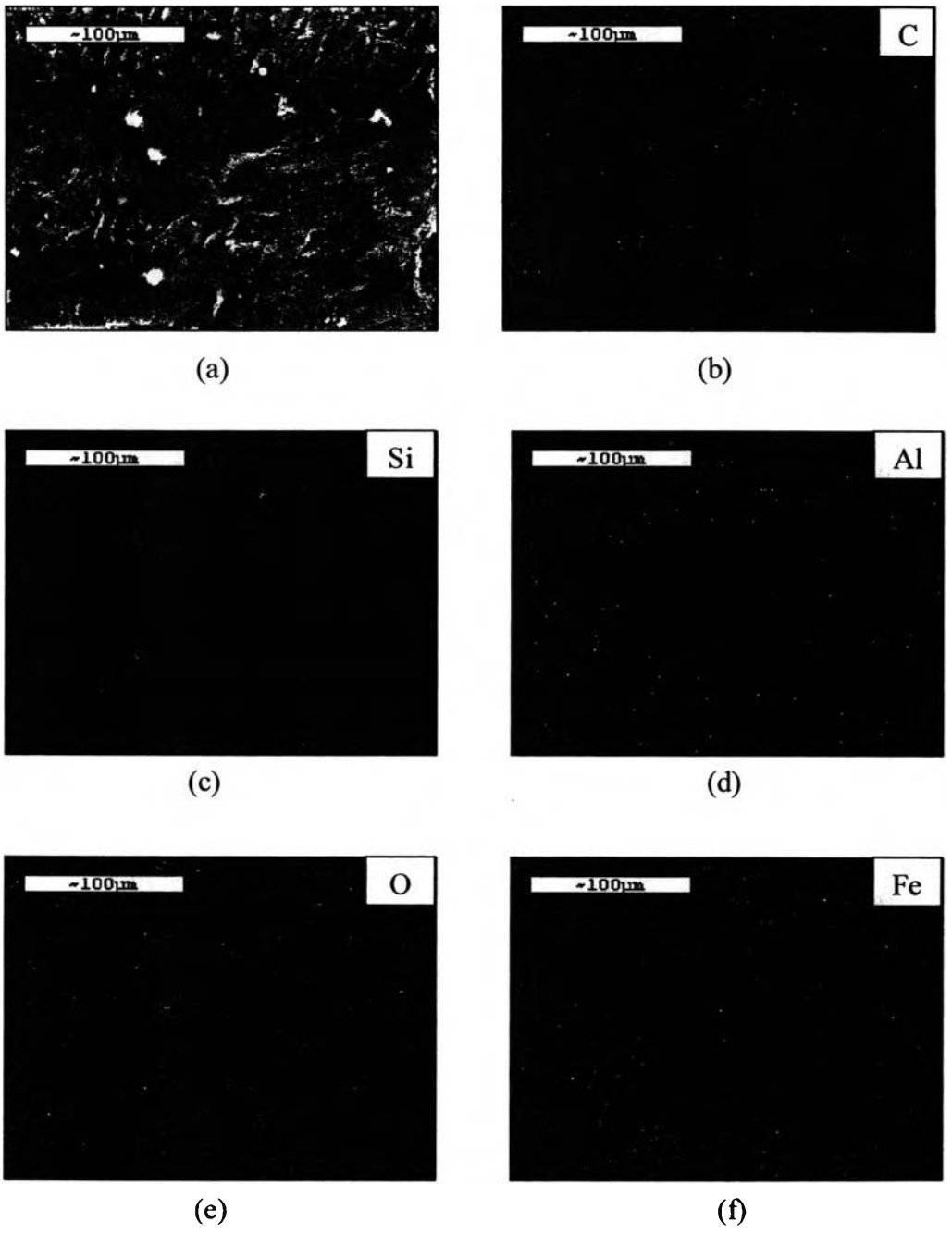

Figure 5.6 SEM image and consistent EDX micrographs of PLA/5% wt PCL/1% wt magnetic PCH (a) SEM image, (b) C mapping, (c) Si mapping, (d) Al mapping, (e) O mapping, and (f) Fe mapping.

Dispersion of magnetic PCH in PLA nanocomposites

The phase separation of the nanocomposites between magnetic PCH and the PLA matrix was studied by scanning electron microscope (SEM). Figure 5.7(b) shows the smooth surface of PLA/5%wt PCL which indicated the good compatible of PCL. At 1%wt of magnetic PCH in PLA/5%wt PCL, the surface was observed homogeneous whereas the roughness of the surface gradually appeared in Figure 5.7(c) which showed the magnetic PCH particles were discernible as white spots.

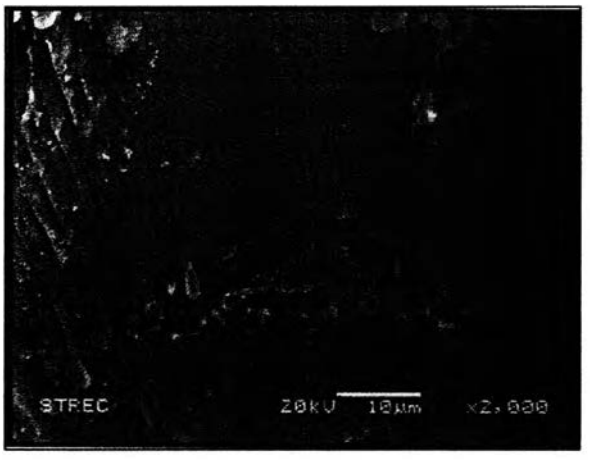

(a)

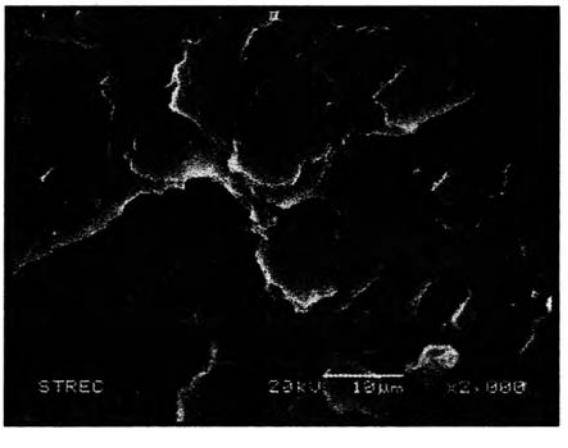

(b)

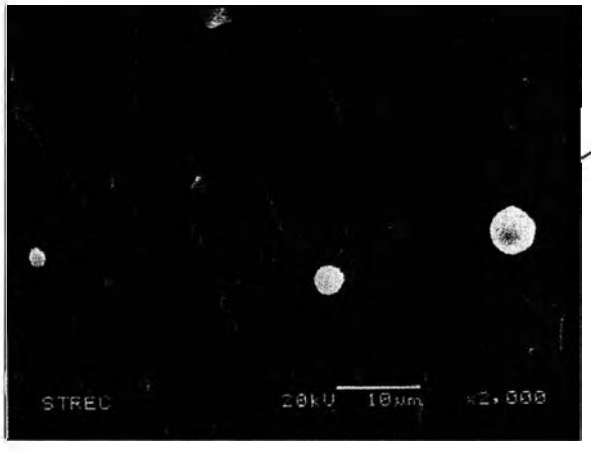

(c)

Figure 5.7 SEM images of PLA nanocomposites (a) neat PLA, (b) PLA/5% wt PCL and (c) PLA/5% wt PCL/1% wt magnetic PCH.

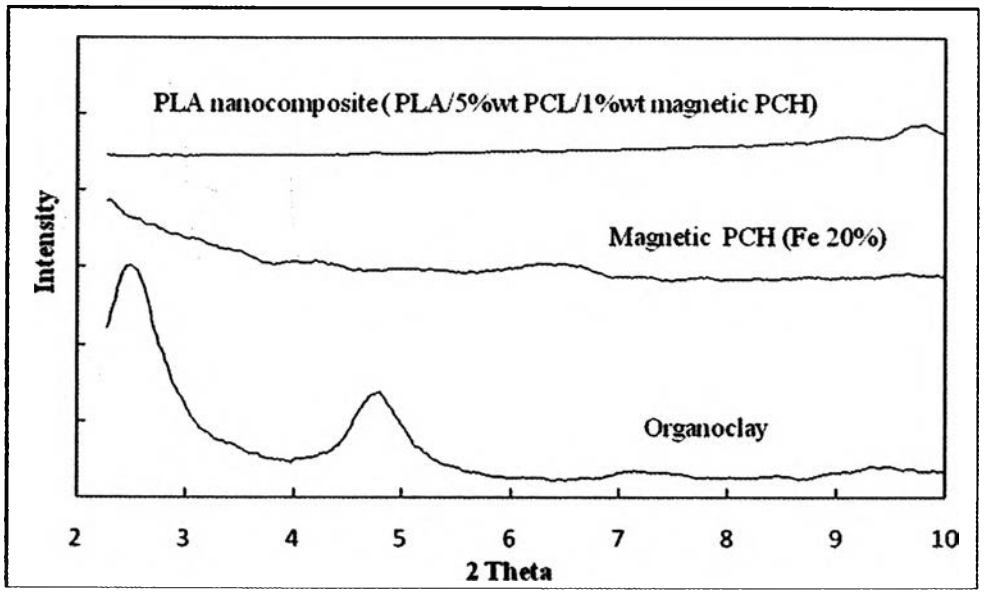

Figure 5.8 The XRD patterns of organoclay, magnetic PCH(Fe20%) and PLA nanocomposite (PLA/5%wt PCL/1%wt magnetic PCH).

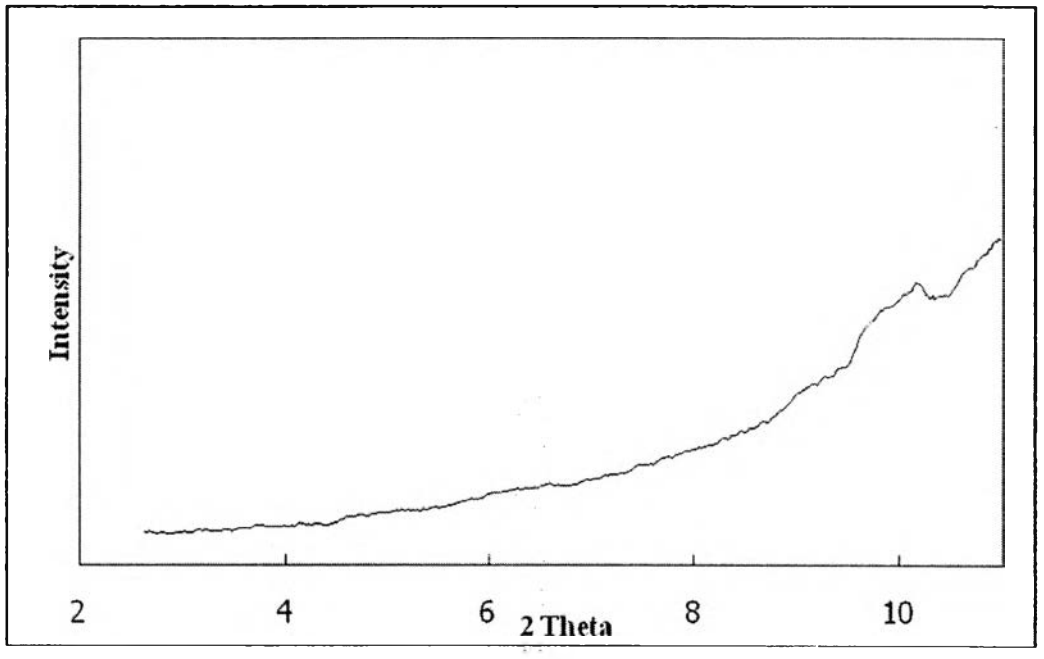

Figure 5.9 XRD patterns of PLA/5% wt PCL/1% wt magnetic PCH.

Figure 5.9 shows the XRD patterns of of PLA/5% wt PCL/1% wt magnetic PCH. The PLA nanocomposite showed the shift to lower angle. This implies that PLA nanocomposites was nearly exfoliated when added 1%wt magnetic PCH [17].

Oxygen Gas permeability of PLA nanocomposites

The migration of gases through materials has been a critical factor in the ability of food packaging to increase the shelf life of products. Generally, the presence of nanoclay (high aspect ratio) in nanocomposites provides the improvement of gas barrier properties due to the hindered diffusion pathways through the nanocomposites [10]. Oxygen gas permeability of PLA, PLA/5%wt PCL and PLA nanocomposite sheets were summarized in Table 5.4. Magnetic PCH improved gas barrier property of the sheet, indicating by lower oxygen gas permeability of the nanocomposite sheet. Improvement in barrier property was due to the presence of magnetic PCH providing tortuous path in the films owing to these materials were combined with micro- and mesoporosity so gas molecules might be induced through these porous structures.

Table 5.4 Oxygen Gas Permeability Rate of PLA, PLA/5%wt PCL and PLA nanocomposites

Sample	Oxygen gas permeability rate ($cc/m^2.d$)
PLA	132
PLA/5% wt PCL	112
PLA/ 5%wt PCL/ 1%wt magnetic PCH	106

Packaging Freshness Test

Magnetic PCH (20%wt of Fe in PCH) exhibited a remarkably significant bacteriostatic effect against *Escherichia coli* and *Staphylococcus aureus* and the PLA/ 5%wt PCL/ 1%wt magnetic PCH showed lower the oxygen gas permeability rate than neat PLA due to barrier properties of the magnetic PCH and magnetic PCH. By combinding result of antibacterial testing and the oxygen gas permeability, 1 %wt magnetic PCH (20%wt of Fe in PCH) blended with PLA and 5%wt PCL were selected as the most suitable for meat packaging as shown in Figure 5.10-5.11. The result showed that PLA nanocomposite can extend shelf life of meat. To use as a freshness indicator, the meat spoilage was indicated by the color changing from initially yellow to finally green [11].

Figure 5.10 Food packaging of (left) PLA/5% wt PCL/1% wt magnetic PCH and (right) neat PLA with 15.50 g chicken at ambient temperature in 4 days.

Figure 5.11 Food packaging of PLA/5% wt PCL/1-4% wt magnetic PCH with 15.50 g chicken at ambient temperature in 4 days.

5.5 Conclusions

Magnetic modified mesoporous clay nanocomposites were prepared from PCH which had the molar ratio of dodecylamine/TEOS was 20/200 and modified by 20%wt Fe ion for magnetic properties. The dispersion of the 1 to 4 wt% magnetic

PCH in PLA matrix was improved by incorporating 5 wt% of PCL as a compatibilizer. Subsequently, they were fabricated to thin sheet by compression molding machine. The thermal properties increased and mechanical properties of PLA nanocomposites decreased with content of magnetic PCH increased. From XRD results, the silicates of magnetic PCH were exfoliated in PLA nanocomposites. The PLA nanocomposite showed lower the oxygen gas permeability rate than neat PLA. Results of antibacterial testing and the oxygen gas permeability showed that PLA nanocomposite can extend the shelf life of meat.

5.6 Acknowledgements

This work is funded by National Research Council of Thailand (NRCT). The authors would also thanks Rachadapiseksompoch and the Center of Excellence for Petroleum, Petrochemical, and Advanced Materials, Polymer Processing and Polymer Nanomaterial Research Unit for their partially funding.

5.7 References

[1] Drumright, R.E., Gruber, P.R., and Henton, D.E Advanced Materials 12 (2000) 1841.

[2] Bax, B., Mussig, J. Composites Science and Technology 68 (2008) 1607.

[3] Rhim, J.W., Hong, S.I., Ha, C.S. Food Science and Technology(2008).

[4] Petersen, K., Nielsen, P.V., Bertelsen, G., Lawther, M., Olsen, M.B., Nilsson, N.H., and Mortensen, G. Trends in Food Science and Technology 10 (1999) 52.

[5] Kikkawa, Y., Fujita, M., Abe, H., and Doi, Y. Biomacromolecules 5 (2004) 1187.

[6] Meneghetti, P. and Qutubuddin, S. Thermochimica Acta (2006) *In Press.*

[7] Arau´jo, E.M., Me´lo, T.J.A., Santana, L.N.L., Neves, G.A., Ferreira, H.C.,Lira, H.L., Carvalho, L.H., A'vila Jr., M.M., Pontes, M.K.G., and Arau´jo, I.S., Materials Science and Engineering B 112 (2004) 175.

[4] Lertwimolnun, W., and Vergnes, B. Polymer 46 (2005) 3462.

[5] Shah, R.K., Hunter, D.L. and Paul, D.R. Polymer. 46 (2005) 2646.

[6] Ishii, R., Nakatsuji, M., and Ooi, K. Micropor. Mesopor. Mater. 79 (2005)

111.

[7] Galarneau, A., Barodawalla, A., and Pinnavaia, T.J. Nature 374 (1995) 529.

[8] Sinha Ray, S., and Okamoto, M. Prog. Polym. Sci. 28 (2003) 1539.

[9] Gu, S.Y., Ren . J., Dong, B. Journal of Polymer Science Part B:Polymer Physics. 45 (2007) 3189.

[10] LeBaron, P.C., Wang, Z., and Pinnavaia, T.J., Applied Clay Science 15 (1999) 11.

[11] Seephueng, A., Magaraphan, R., Nithitanakul, M., and Manuspiya, H. Proceeding of the 14 th PPC Symposium on Petroleum, Petrochems, and Polymers, (2008).

[12] Polverejan, M., Liu, Y., and Pinnavaia, T.J. Chem. Mater. 14 (2002) 2283.

[13] Zhu, H.Y., Ding, Z., and Barry, J.C. J. Phys.Chem. B. 106 (2002) 11420.

[14] Ramos Filho, F.G., Melo, T.A., Rabello, M.S., and Silva, S.M., Polymer Degradation and Stability 89 (2005) 383.

[15] Perrin-Sarazin, F., and Ton-That, M.T., Bureau, M.N., and Denault, J., Polymer 46 (2005) 11624.

[16] Modesti, M., Lorenzetti, A., Bon, D., and Besco, S. Polymer Degradation and Stability 91 (2006) 672.

[17] Alexandre, M. and Dubois, P. Materials Science and Engineering 28 (2000) 63.